Desmodesmus sp. pigment and FAME profiles under different illuminations and nitrogen status

Victor Pozzobon, Wendie Levasseur, Cédric Guerin, Nathalie Gaveau-Vaillant, Marion Pointcheval, Patrick Perre

Desmodesmus sp. pigment and FAME profiles under different illuminations and nitrogen status

Victor Pozzobon [1*]

Wendie Levasseur [1]

Cédric Guerin [1]

Nathalie Gaveau-Vaillant [2]

Marion Pointcheval [1]

Patrick Perré [1]

[1] LGPM, CentraleSupélec, Université Paris-Saclay, SFR Condorcet FR CNRS 3417, Centre Européen de Biotechnologie et de Bioéconomie (CEBB), 3 rue des Rouges Terres 51110 Pomacle, France

[2] Résistance Induite et Bioprotection des Plantes - RIBP (EA 4707), Université de Reims Champagne-Ardenne, Reims, France

* Corresponding author: victor.pozzobon@centralesupelec.fr

Abstract

Acknowledging the limited knowledge available on microalgae *Desmodesmus sp.*, a specimen isolated from nearby freshwater lake was studied. Photobioreactor runs were led at two different illuminations (moderate - 150 µmolPhotonPAR/m²/s - and high - 300 µmolPhotonPAR/m²/s) and under three nitrogen status: sufficient, deficient and starved. Pigment and FAME profilings were carried out. *Desmodesmus sp.* has a Chlorophyceae common pigment profile with natural occurrence of lutein. Nitrogen deficiency induced both chlorophyll *a* and *b* contents decrease while not modifying the overall profile. Long term starvation induced pigment profile modification: disappearance of violaxanthin and stronger expression of carotenoids such as canthaxantin. FAME profiling showed that the three major fatty acids produced by this strain are oleic (7.0 %g/gDW), linoleic (5.0 %g/gDW) and γ-linolenic (6.9 %g/gDW) acids. The first two being the storage lipids of this strain. Those two fatty acids have valuable health properties and may pave the way toward nutraceutics covalorization.

Keywords

Desmodesmus sp., Covalorisation, Pigment, FAME, Profiling

1. Introduction

Microalgae started to draw scientists and engineers attention about 50 years ago for many reasons. The most striking ones being: photosynthesis, robustness and fast growth. In more details, while growing, microalgae can derive their energy from sunlight and fix inorganic carbon. Furthermore, compared with higher plants they show superior photosynthetic efficiencies 4-5 % (compared with 1-2 %) (Walker 2009), no intrinsic sensibility to seasonality and faster growth. Another

edge of microalgae is that their culture can be deployed on non-agricultural land, without pesticides and using wastewater. Thanks to all this, it is nowadays commonly admitted that microalgae can be of help in facing the numerous challenges mankind is confronted with. Among them climate change, induced by fossil carbon release, may be the most urging one. As part of the solution, microalgae can sequestrate atmospheric carbon dioxide, mitigate its emissions, and be a substrate of choice for third generation biofuel (Sati et al. 2019).

Still, after years of research, the scientific community acknowledged the fact that the sole production of biofuel is not viable economically (Rizwan et al. 2018). Indeed, even in the most optimistic scenarii, whole biomass cost is about 0.82 €/kg dry weight (Acién Fernández et al. 2019). Thus biofuel production will only be possible as part of a co-valorization process of microalgal biomass. Several strategies can be envisioned: growing biomass on formulated wastewater (alleviating 0.20 €/kg dry weight (Acién Fernández et al. 2019)) or extracting high added-value molecules before turning spent biomass into biofuel.

In addition to this paradigm shift, strain selection and optimization will also be key (Lim et al. 2017), as it would ease the lifting of the three bottlenecks of microalgae large scale cultivation: dense culture (as cultures only contain only 1 - 20 g/l) (Enamala et al. 2018), harvest (Fasaei et al. 2018), extraction (Rizwan et al. 2018). Luckily only a fraction of the microalgae species have been discovered (Guiry 2012), and even fewer studied. That is why, with this in mind, researchers have led environmental surveys and strain characterization - the initiative of the National Alliance for Advanced Biofuels and Bioproducts being of note. In their work, Neofotis et al. pointed out that, even though widespread, *Desmodesmus* genus is far from well-known and may hide potential for biofuels and bioactive molecules production (Neofotis et al. 2016). This can be confirmed by a simple analysis of Web of Science database. In the date of the 28th of January 2020, topic search for

Chlorella genus yielded 13732 articles, *Scenedesmus* 4979 and *Desmodesmus* only 417. Thus, the present work aims at gaining general knowledge about *Desmodesmus* genus when it comes to its growth rate, medium affinity, pigment and Fatty Acids Methyl Ester (FAME) profiles.

To do so, a *Desmodesmus sp.* strain was isolated from nearby lake. Indeed, obtaining strains from closeby ponds ensures that they are already adapted to local light and temperatures conditions. Hence it would ease local deployement in case of promising discovery. After collection, this strain response to varying growth media was screened. Then, its pigment and FAME profiles were extracted. This was done under different growth conditions as microalgae are known to be able to adapt such profiles depending on environmental conditions (Ratha et al. 2012). Nitrogen limitation or starvation are techniques frequently applied to microalgae to manipulate their secondary metabolites profiles. For example, Pancha et al. demonstrated that nitrogen limitation leads to a decrease of photosynthetic activity while triggering highest lipid and carotenoid production (Pancha et al. 2014). Similar findings have been reported by many other authors, thus those can now be considered as routine culture protocols (Lari et al. 2016; Mandal et al. 2009; González-Garcinuño et al. 2014; Ratha et al. 2012). Lighting strategies have also be shown to impact microalgal growth. In this regard, the pionneering work of Myers and Kok has to be acknowledged (Kok 1953; Phillips et al. 1954). More recently, excess light has been shown to modify both lipid and pigment profiles (Leonardi et al. 2019; Gris et al. 2014; Sarat Chandra et al. 2017; Sforza et al. 2014). Carotenoids and other xantophylls pigments are expressed as a means to protect the cell from upset photosynthesis induced Reactive Oxygen Species (ROS) (Müller et al. 2001; Choudhury et al. 2001). Thus, after determining the most promising growth medium, *Desmodesmus sp.* pigment and FAME profiles

were determined under nitrogen sufficient, nitrogen deficient as well as moderate and high light conditions.

2. Materials and methods

2.1 Strain

The strain was obtained by sampling in late Autumn 2018 from freshwater Bazancourt lake (GPS: 49.365412, 4.162591), France. Microscope examination confirmed the presence of *Chlorella sp.*, *Scenedesmus sp.*, *Desmodesmus sp.*, *Dunaliella sp.*, *Euglenozoa sp.*, several protozoa and bacteria. The obtained consortium was cultured over BG-11 (Blue-Green medium with 11 elements) medium in 250 ml flasks (50 ml culture medium). Then Petri dish isolation was conducted. From the obtained strains, *Desmodesmus sp.* was latter purified and kept axenic.

With the help of Hegewald pioneering work (Hegewald et al. 2005), the strain was further characterized. Two key factors were used: population distribution and microscopy similarities. This strain population exhibits 2, 4 and 8-cell colonies (Fig. 1, right). Even though cells were extensively observed, no singled cell colonies nor 16-cell colonies were found. The most common ones being the 4-cell colonies, when no stress, nor synchronization is applied (Ševčíková et al. 2013). All of the colonies featured distinguishable long spines, while short spines could not be identified with certainty using benchtop optical microscope. Thus additional observations were carried out with a confocal microscope (Alpha 300 R+ Witec) in order to obtain observations whose focal plan matches the spines position. Those observations revealed the presence of short spines in addition to the long ones (Fig. 1, left). The fact that the strain possesses both short and long spines points towards *Desmodesmus* genus while the types of observed colonies

narrow it down to *pleiomorphus* species. Still, not being taxonomists, the authors would remain cautious and referred to the strain as *Desmodesmus sp.*.

The generation process of this genus is similar to other colony living genus, such as *Scenedesmus*. Generation takes place in an independent manner within each cell composing the colony. When a cell enter the autosporulation process it will form either a 2, 4 or 8-cell colony, depending on the environmental conditions and not on the number of cells present in its current colony. Then, the newly form colony departs from its former host, leaving an empty spot. Finally, manipulation of the light photoperiod allows to select which type of colonies are expressed by the strain (Ševčíková et al. 2013).

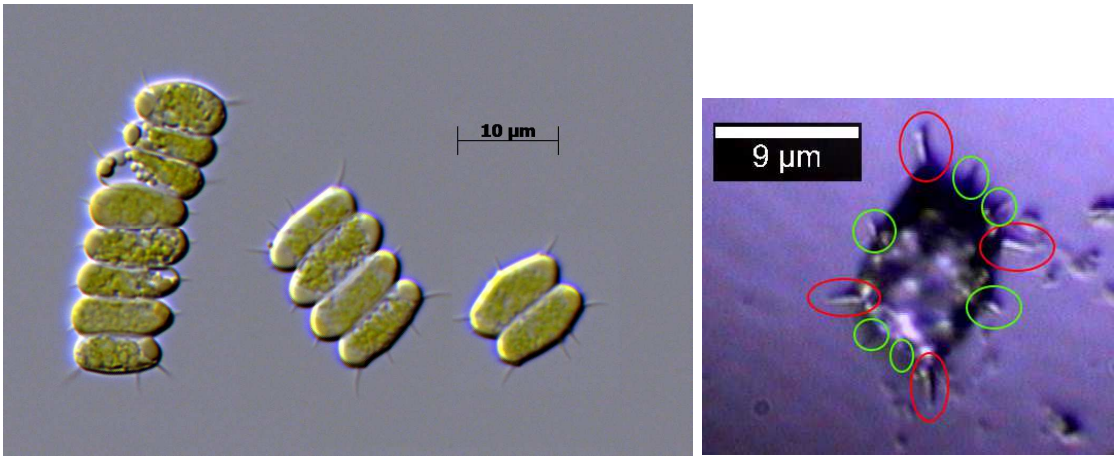

Fig. 1: Visual observations of the Desmodesmus sp. strain used for this study. Sampled from a subculture Right: Microscope observations, magnification x100 (image manipulation: contrast enhancement). Left: Confocal observations. Circled in red: long spines. Circled in green: short spines

2.2 Subculturing

The first action was to identify optimal growth medium for this strain. To do so, Fraquil, WC (Wright's Cryptophyte), BBM (Bold's Basal Medium), B3N (BBM with 3 times more nitrates) and BG-11 media were screened. Those media were

selected as they are indicated for *Scenedesmus* genus growth in Andersen media compendium (Andersen et al. 2005). The second criterium of choice was the range of nitrogen contents those media offered (from 0.10 mM for Fraquil to 17.6 mM for BG-11)

In order not to bias the screening by former BG-11 subculturing, the strain was subcultured on each medium for three weeks. Three passagings consisted in a 100-fold dilution to 50 ml of culture medium in 250 ml flasks. Illumination was set as 75 µmolPhotonPAR/m²/s and temperature at 20 °C. They were all conducted in triplicates. Fraquil medium showed sign of early exhaustion and was therefore excluded from the screening. Cell concentration was tracked after a fourth passaging, in triplicate again. The monitoring was realized twice daily, optical density at 750 nm (OD_{750} hereafter) was used as proxy of cell concentration (more details are available in Sec. 2.4).

Media screening are detailed in Section 3.1. Briefly, B3N was the most suited medium and was therefore used for subculturing during the remaining of this study. Subculturing took place every Monday morning, with unchanged passaging procedure: 1/100 sampling, 250 ml flasks, 50 ml culture medium, 75 µmolPhotonPAR/m²/s, 20 °C, duplicate. Once per month, culture plated on glucose enriched Lysogeny Broth (LB, promoting bacteria proliferation) to check for potential mother culture contamination. None were found.

2.3 Culture protocol

The culture was fed in a 2.5-liter bubble column photobioreactor. Such a large vessel was used for two reasons. First of all, it is closer to industrial scale culture protocols than large capacity shake flasks. Second, it allows for large sampling volumes, meaning that, for every sample, enough biomass is collected to later process it and acquire both pigment and FAME profiles. External lighting was

ensured by cool white LED ribbons (OSRAM GW JDSRS1.EC) placed all around the photobioreactor. LEDs were closely packed together across all the photobioreactor height to ensure uniform illumination. Lighting capacity ranges from 30 to 300 µmolPhotonPAR/m²/s at the surface of the culture. In addition, as it is known that light spectrum influences microalgae (Mohsenpour et al. 2012), light spectra were acquired across this range (Ocean Optics Flame-T-UV-Vis portable spectrophotometer). Light spectrum exhibits no variation over the aforementioned range. Finally, culture temperature is controlled using a heater-chiller directly injecting water into the thermal jacket.

The cultures were led with 2 liters of B3N medium. Aeration was set at 0.2 vvm, with 2.5 % CO_2-enriched air. Culture temperature was set at 20 °C. Two different illuminations were tested 150 and 300 µmolPhotonPAR/m²/s. The first one represents moderate illumination, at least for the resembling *Scenedesmus* genus (Liu et al. 2012; Přibyl et al. 2016) while the second should trigger light stress. Inoculation was realized after sterilization by injecting 50 ml of B3N subcultured cells passaged 10 days before. This delay was chosen to ensure that cells were in the exponential phase at the time of inoculation. At the end of each run, the remaining culture was removed and the photobioreactor cleaned and sterilized.

Finally, long term nitrate starvation effects were also explored. Sadly, despite the fact that a liter size capacity photobioreactor was used in this study, this volume was still to low to allow for one month or more follow-up (with at least 120 ml withdrawn each day). Thus shake flasks subcultures, without continuous sampling, were used for this last part of our investigation. To do so, subcultures were left under incubation conditions (75 µmolPhotonPAR/m²/s, 20 °C, air). They were analyzed one month after passaging.

2.4 Cell concentration monitoring

Samples were drawn out of the culture vessel twice daily, 1 ml for shake flasks, 50 ml for the photobioreactor (discarding the 10 first milliliters). Cells growth was monitored using optical density (Shimadzu UV-1800 spectrophotometer) as proxy of cells dry weight. Samples were diluted to an optical density of 0.4 or less before recording the value. Following Griffiths' advices (Griffiths et al. 2011), the optical density was acquired at 750 nm, as it allows to almost only account for cell walls and not pigments, hence measuring only for biomass. Once more, following his recommendations, a calibration curve linking optical density and dry weight was produced using late exponential phase cells (7 points, range: 0.02 to 0.5, R^2 = 0.997). With this curve it is possible to compute biomass density from optical density readings. Finally, offline pH measurements and frequent microscope observations were done to check the cells condition.

2.5 Nitrate concentration monitoring

As nitrogen is known to have a dramatic impact on cell conditions, nitrate concentration was monitored until exhaustion. Samples were prepared by centrifugation (11000 rpm, 4 °C, 10 min, Eppendorf 5804 R). Supernatant was then filtered (0.22 µm polypropylene) before being diluted with milliQ water (Integral-5, Merck, also analyzed for correction) in order to be in the range of 0.2 to 10 mg/l. Nitrate quantification was carried out on an ICS-5000+ Ion Chromatography system (Thermo Fisher Scientific) coupled with a conductivity detector. Separation was achieved on an AS11-HC column (2x250 mm, 4 µm) protected by a guard column AG11-HC (2x50 mm, 4 µm). Column temperature was maintained at 35 °C. The mobile phase of 30 mM of potassium hydroxide was at a flow rate of 0.2 mL/min in isocratic mode and was delivered by an EGC 500 eluent generator. The eluent generated was then purified by a CR-TC to trap

impurities such as carbonate. The suppressor was an ADRS 600, 4 mm, operated in recycle mode at 15 mA. The injection volume was 2 µL and total run analysis lasted 30 minutes. Nitrate was identified by comparison of its retention time with standard solutions. Quantification was achieved using the height of the peak in external calibration (0.2 to 10 mg/l range). Nitrate standard was purchased from Sigma-Aldrich with a TraceCert quality which is a standard at 1000 ± 4 mg/l.

2.6 FAME profile determination

Transesterification done using an in-situ transesterification following NREL protocol (Van Wychen et al. 2013). Quantification of the FAME was carried out on a GC-2010 Plus coupled to a GCMS-TQ8040 triple quadrupole mass spectrometer (Shimadzu). Separation was achieved on a HP-88 capillary column, 100m x 0.25 mm x 0.20 µm (Agilent). Helium (99.9999 %) was used as the carrier gas with a column flow rate of 2 mL/min, the linear velocity was kept constant during the analysis. The injection volume and temperature were 1 µL and 240 °C, samples were injected in splitless mode. The oven temperature started at 50°C for 1 minute and raised to 180°C with a rate of 20 °C/min, held for 5 minutes. It was successively raised with a rate of 10 °C at 200, 210, 220 and 230 °C and respectively for 5,5,1 and 6 minutes. Total run time was 34.5 minutes. Detection was done by the triple quadrupole in Electron Ionisation (EI) with an energy of 70 eV. The temperature of the ion source was set at 200 °C and the interface at 210 °C. The acquisition was done in MRM mode (Multiple Reaction Mode), transitions and energy of collision for each FAME are supplied in the supplemental material section. Compounds were identified by comparison with their retention time with standards, for each compound 3 different transitions were recorded, one was used for quantification using the area of the chromatographic peak and the two others were used as qualifiers. The ratio of intensity between quantifiers and qualifiers was also used for additional identification. Internal

calibration was done using C13:0 as the internal standard. FAME standard was the Supelco 37 component FAME mix, CRM47885 from Sigma-Aldrich. All samples were also acquired in scan mode using the third quadrupole from 50 to 400 m/z in order to visualize any unquantified compound.

2.7 Pigment profile determination

Samples were prepared by centrifugation of 50 ml of culture (4 °C, 11000 rpm, 10 min). Supernatant was used for nitrate quantification. The pellet was frozen, then freeze-dried (1 day primary drying, 2 days secondary drying, Christ alpha 1-2 LD +). 1 mg of dried microalgae powder was homogenized in 5 ml pure methanol using MP Biomedicals FastPrep42 bead miller. Liquid was then filtered (0.22 µm) and stored in dark vials at 4 °C before quantification.

Quantification of pigments were carried out on an Ultima 3000 HPLC (Thermo Fisher Scientific) coupled with an UV Detector. Separation was achieved on an Acclaim Polar Advantage II C18 column (4.6 x 150 mm, 3 µm, 120 Å) from Thermo Fisher Scientific. Column temperature was maintained at 30 °C. Pure methanol was the mobile phase, the flow rate was 0.5 mL/min and the elution set in isocratic mode. Injection volume was 5 µL and the total run analysis was 40 minutes. Compounds were identified by comparison of their retention time and of their UV-Vis spectra with standard solutions. UV-Vis spectra were recorded from 200 nm to 700 nm, absorbance was recorded at 400, 450, 500 and 650 nm. Pigments quantifications were done at 650 nm. It was achieved using the area of the peaks in external calibration, which concentrations ranged from 0.25 to 5 mg/l. Pigment standards and methanol were purchased from Sigma-Aldrich. Standards had a purity greater than 97 %.

2.8 PAM measurement

In order to assess for the state of the photosynthetic apparatuses, chlorophyll fluorometry analyses were carried out during the exponential phase under nitrogen sufficient conditions. Experiments were led using pulse modulated spectrophotometer (Dual-PAM-100, Walz). Two types of measurement were conducted. First Fv/Fm ratio was analysed, as it is an efficient proxy of photodamage. Even though fast and informative, Fv/Fm ratio can be seen as a too simplistic description of photosynthetic apparatuses. Indeed, for this measurement cells are dark adapted and exposed to only one flash. Hence this specific measure does not yield information on actinic light management under different illuminations. Still, it would detect severe damage done to the photosynthetic apparatuses.

Thus, to avoid this shortfall, photosystem II yield (Y(II)) and NPQ yield (Y(NPQ)) were also recorded for 3 different actinic light intensities: 126 µmolPhotonPAR/m²/s, to mimic the first photobioreactor conditions (150), 339, to mimic the second condition (300) and 1028 to investigate the cell reaction to excess light. Y(II) indicates the fraction of energy that is processed by the non-cyclic photosynthesis scheme, hence driven towards carbon fixing. Y(NPQ) quantifies the fraction of incident light energy that is safely regulated via xanthophyll cycle.

Each measurement point was triplicated.

3. Results

3.1 Media screening

Media screening results are presented in Figure 2. As one can see, standard deviations are very low and results are statistically significantly different from medium to medium. The highest growth rate was obtained with B3N (0.0389 ± 0.001 h^{-1}) followed by BBM (0.0313 ± 0.003 h^{-1}), BG-11 (0.0271 ± 0.0004 h^{-1}) and WC (0.0184 ± 0.001 h^{-1}). This observation calls for a comment on strain affinity towards nitrogen. Indeed, WC, BBM, B3N and BG-11 show increasing nitrogen contents, and relatively similar composition for the last three of them. This means that the 3-fold increase in nitrogen content from BBM to B3N is favourable to this strain. On the other side, the same 3-fold increase from B3N to BG-11 exhibits detrimental effect. Thus, an optimal nitrogen concentration exists, probably not too far from B3N concentration.

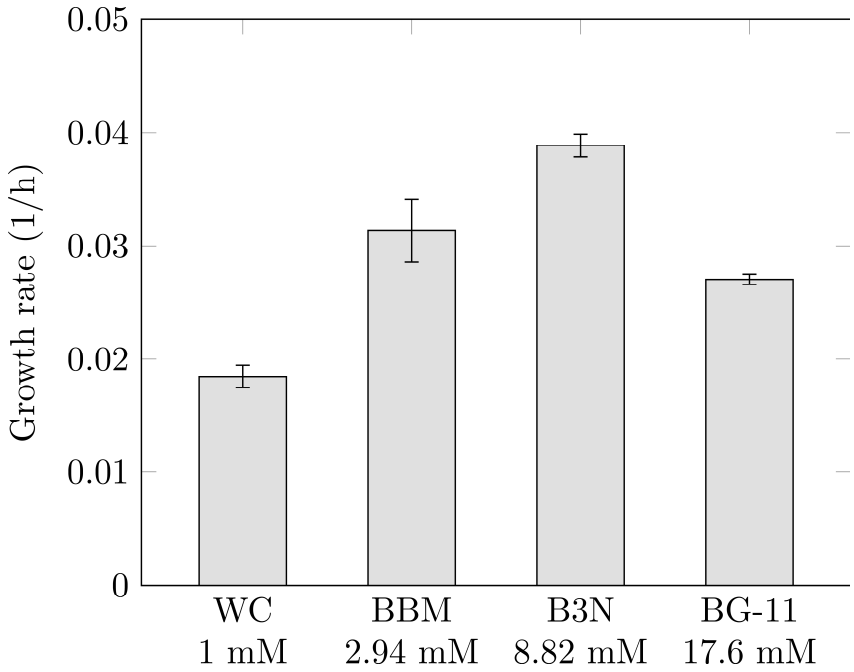

Fig. 2: Growth rates resulting from the media screening. First abscissa line: media names, second abscissa line: nitrogen content. Error bars: standard deviation (n=3)

3.2 Cell growth, substrate monitoring and photosynthetic status

Shake flask and photobioreactor runs unfolded as expected. Repeatability was very good for moderate illumination runs (growth rates of 0.0460 and 0.0463 h^{-1}, exponential phase log fit $R^2 > 0.97$ for both runs) and reasonably for high illumination ones (growth rate of 0.0174 and 0.0153 h^{-1}, $R^2 > 0.98$ for both runs). Thus, only one run will presented and commented hereinafter.

Figure 3 presents the follow up of the first 150 µmolPhotonPAR/m²/s photobioreator run. Culture started with a lag phase (0 to 72 h), followed by an exponential phase (72 to 129 h), a linear phase (129 to 241 h) and a stationary phase. Nitrate concentration exhibited a classical behaviour: almost plateau during the lag phase, with a value close to the one of the virgin medium, then a sharp decrease during the exponential phase. One should note that nitrate exhaustion and exponential phase end took place at the same time. Finally, over the culture, pH rose from 6.3 to 7.6 at the end of the run.

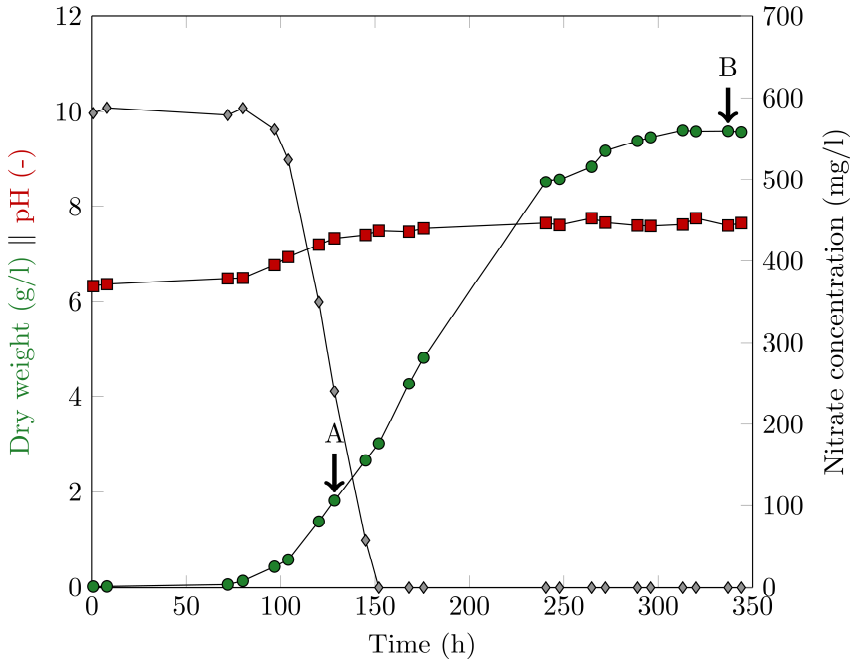

Fig. 3: 150 µmolPhotonPAR/m²/s photobioreator run monitoring. Green markers: biomass concentration. Red markers: pH. Grey markers: nitrate concentration. A mark: nitrogen sufficient sample, B mark: nitrogen deficient sample

Thanks to those curves, it was possible to determine the samples produced in nitrogen sufficient conditions and those produced under nitrogen depletion. Nitrogen sufficient samples were taken in exponential phase, while nitrogen was still available. Nitrogen limited samples were taken in late exponential (early stationary) phase. Once identified those samples were used for pigment and FAME profiling. Thus 5 profiles have been established: 150 µmolPhotonPAR/m²/s nitrogen sufficient and deficient, 300 µmolPhotonPAR/m²/s nitrogen sufficient and deficient and 75 µmolPhotonPAR/m²/s nitrogen starved for 1 month.

Finally, chlorophyll fluorometry results are available in Figure 4. They are displayed as the energy flux repartition: Y(II) energy flux forwarded from PSII to PSI, Y(NPQ) safely regulated energy excess, Y(NO) the remaining energy *i.e.* unregulated energy excess (Y(NO) = 1 - Y(II) - Y(NPQ)) . They were obtained during the exponential phase under nitrogen sufficient conditions on the replicate runs. In addition, Fv/Fm ratio was 0.778 ± 0.038 for the culture under 150 µmolPhotonPAR/m²/s and 0.570 ± 0.059 for the one under 300 µmolPhotonPAR/m²/s .

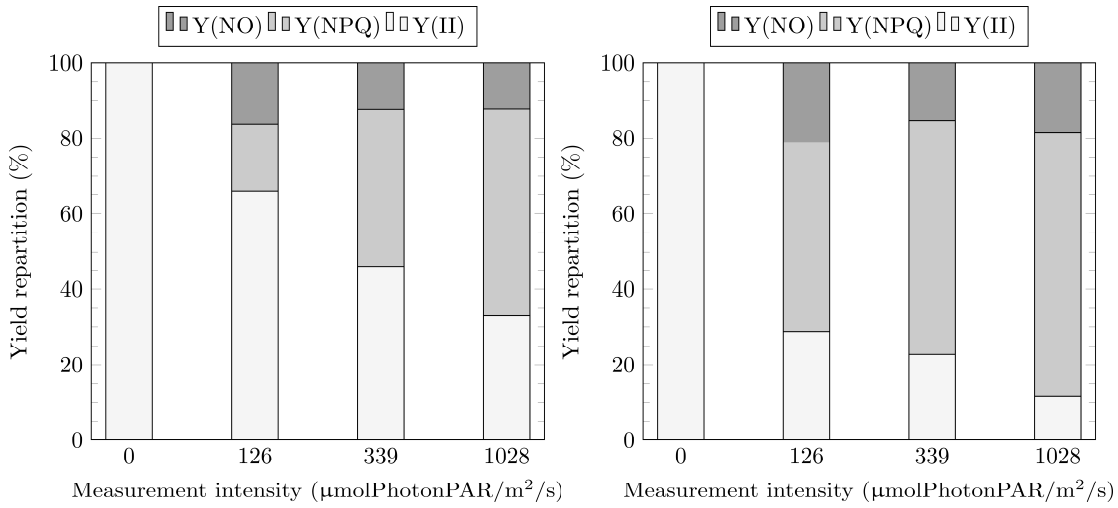

Fig. 4: PAM measurements for both lighting conditions (left: 150 µmolPhotonPAR/m²/s, right: 300 µmolPhotonPAR/m²/s). Samples taken in exponential phase, nitrogen sufficient part. Standard deviation (n=3) below 0.06

3.3 Pigment profiles

First of all, pigment profiles were very repeatable from one run to the other. 150 µmolPhotonPAR/m²/s and 300 µmolPhotonPAR/m²/s photobioreactor yielded similar profiles, with different relative amounts of pigment species. Furthermore, the two growth conditions exhibited the same trend when going from nitrogen sufficient to nitrogen deficient phase. Over 1-month starvation, the culture turned

from green to orange/red color. From these profiles, four pigments can be identified with certainty in most of the conditions: chlorophyll *a*, chlorophyll *b*, lutein and violaxanthin. Other pigments, such as asthaxanthin and canthaxanthin have been detected in some samples, still their contents were too low to be quantified or even identified with certainty in all samples. Finally, the four main pigment contents have been quantified and are reported in Table 1

Table 1: Major pigments quantification results for the five growth conditions. BQL: Below Quantification Limit. LoQ: Limit of Quantification. LoD: Limit of Detection. Displayed as value ± measurement uncertainty

		Pigment content (%g/gDW)			
Conditions		Chl *a*	Chl *b*	Lutein	Violaxanthine
150 µmolPhotonPAR/m^2/s	N sufficient	1.498 ± 0.016	0.694 ± 0.035	0.251 ± 0.005	0.113 ± 0.002
	N deficient	0.187 ± 0.003	0.131 ± 0.004	0.148 ± 0.003	< LoQ
300 µmolPhotonPAR/m^2/s	N sufficient	1.427 ± 0.014	0.638 ± 0.032	0.244 ± 0.005	0.097 ± 0.002
	N deficient	0.838 ± 0.009	0.432 ± 0.018	0.185 ± 0.004	0.076 ± 0.001
1 month old subculture		0.076 ± 0.000	0.031 ± 0.001	0.039 ± 0.000	< LoD

3.4 FAME profiles

Like for the pigments, FAME profiling is very repeatable. Still, while the detected species list does not evolve much, relative amounts of fatty acids vary over the tested conditions. Quantification of the seven major fatty acids is presented in Table 2. As one can see, going from nitrogen sufficient to nitrogen deficient condition triggered oleic acid accumulation. This trend is exacerbated by nitrogen starvation. Furthermore, nitrogen starvation also promotes storage of palmitic acid. In addition to nitrogen status manipulation, light stress induction also had an

impact on the strain FAME profile. Going from 150 to 300 µmolPhotonPAR/m²/s reduced by a factor almost two the quantities of oleic and linoleic acids. Finally, total fatty acid content is also computed on the last row of the table. As one can see 1 month nitrogen starvation allowed the strain to accumulate a twofold quantity fatty acids compared with photobioreactor runs. This behavior, which mainly supported through palmitic and oleic acids production, is thought to be the origin of the appearance of the culture orange/red color.

4. Discussion

4.1 Light stress assessment

The first step was to ensure that 300 µmolPhotonPAR/m²/s illumination could actually be considered as a light stress condition while 150 µmolPhotonPAR/m²/s illumination should not be.

380 *Table 2: Major fatty acids quantification results for the five growth conditions. LoD: Limit of Detection. Displayed as value ± measurement uncertainty*

	Conditions	150 µmolPhotonPAR/m²/s		300 µmolPhotonPAR/m²/s		1 month old subculture
		N sufficient	N deficient	N sufficient	N deficient	
Lipid content (%g/gDW)	Palmitic acid (C16:0)	0.527 ± 0.011	0.665 ± 0.014	0.449 ± 0.010	0.615 ± 0.013	1.624 ± 0.036
	Heptadecanoic acid (C17:0)	0.049 ± 0.001	0.054 ± 0.001	0.035 ± 0.000	0.078 ± 0.001	0.148 ± 0.003
	Stearic acid (C18:0)	< LoD	0.194 ± 0.004	< LoD	0.044 ± 0.001	0.252 ± 0.005
	Cis-9-oleic acid (C18:1n9c)	0.979 ± 0.023	2.762 ± 0.064	0.307 ± 0.007	1.142 ± 0.026	6.959 ± 0.164
	Linoleic acid (C18:2n6c)	2.070 ± 0.048	2.312 ± 0.054	0.915 ± 0.021	0.742 ± 0.017	5.027 ± 0.119
	Arachidic acid (C18:3n6)	0.105 ± 0.002	0.099 ± 0.002	0.063 ± 0.001	0.095 ± 0.002	0.158 ± 0.003
	γ-linolenic acid (C18:3n3)	6.461 ± 0.152	4.322 ± 0.101	6.819 ± 0.160	6.663 ± 0.156	6.865 ± 0.162
	Total	10.21	10.42	8.61	9.40	21.14

On one hand, 150 µmolPhotonPAR/m²/s illumination runs yielded the same growth rate as B3N medium screening (around 0.0460 h^{-1}, under 75 µmolPhotonPAR/m²/s). Light, as any substrate has a 3-phase impact on culture: 1. affinity phase - growth rate linear increase, 2. plateau phase - stable growth rate, 3. inhibition - growth rate decrease (Ohad et al. 1990). The fact that subculturing and moderate light runs yielded the same growth rate is a token of fact that both were led in the plateau phase, hence no light limitation nor inhibition. This is confirmed by the value of the Fv/Fm ratio (0.778 ± 0.038) which indicates proper functioning of the photosynthesis apparatus. Indeed, a value of 0.8 indicates a fully photosynthetically capable culture, while the culture is still considered 'healthy' down to 0.6 (Masojídek et al. 2003).

On the other hand, 300 µmolPhotonPAR/m²/s illumination runs yielded a lower growth rate (0.0174 h^{-1}). In addition, photosynthetic apparatus analysis indicated a hindered Fv/Fm ratio of 0.570 ± 0.059. This could be further investigated using yields measurements (Fig. 4). Both cultures exhibit the same trend, a decreasing Y(II) with increasing light. Still lower values are reported for the high illumination culture. An important difference is highlighted under 1028 µmolPhotonPAR/m²/s. In this case the moderately illuminated culture photosystems II forward about 33.1 % of incoming energy, while the highly illuminated cultures only 11.6 %. Photosystems II energy forwarding at this illumination level is harmful for the whole photosynthetic apparatus on the long run (more than 20 minutes) (Baroli et al. 1998). In time, it will induce severe damages. Thus a low Y(II) under excessive illumination shows that the strain has adapted and diverts energy toward the NPQ mechanisms. This is validated by the Y(NPQ) values which clearly indicate that the strain grown under high light is consistently more efficient at safely disposing excess energy. All this shows that the cells cultured under 300

µmolPhotonPAR/m²/s illumination have deployed a strategy to cope with high light.

All in all this validates the occurrence of light stress under 300 µmolPhotonPAR/m²/s which is not the case under 150 µmolPhotonPAR/m²/s. Still this stress is not doing excessive harm to the photosynthetic apparatuses and cannot be referred to as photodamage. With this in mind, the results will be further discussed, first by commenting profiles obtained under nitrogen sufficient then nitrogen limited conditions.

4.2 Pigment profile

The photobioreactor obtained pigment profiles are quite common among Chlorophyta phylum. Indeed, they exhibit the two main pigments chlorophyll *a* and *b* in large quantities. In addition, natural occurrence of lutein is observed. Lutein is a primary photosynthetic carotenoid pigment widening light absorption spectrum (Gong et al. 2016). This characteristic is also shared by resembling *Scenedesmus* genus (Wiltshire et al. 2000). No major difference is observed in the pigment profile between the two light conditions. Even though, 300 µmolPhotonPAR/m²/s induces light stress, no carotenoid overexpression is detected. This may suggest that pigment profile modification would have required higher illumination.

On the contrary, nitrogen deficiency had an impact on cell pigment content. While it did not modify the profile per se, nitrogen deficiency strongly decreased the total amount of pigments per cell. Indeed, when confronted with nitrogen limitation cells break down nitrogen containing materials, such as chlorophyll molecules, to redirect nitrogen towards growth metabolism (Adams et al. 2014). Concomitantly, lutein content also decreased. Lutein does not contain nitrogen, still this fall can be explained by the nature of this pigment. As less chlorophylls molecules are

present, only a reduced number of antenna can have their absorption spectrum widened.

Finally, long term nitrogen starvation altered the cell pigment profile. Chlorophyll *a* and *b* as well as lutein contents reached very low levels. Violaxanthin is lacking from this profile (confirmed by a second analysis). Furthermore potent antioxidant carotenoids are detected (canthaxanthin and astaxanthin, β-caroten absence is thought to come from its very apolar nature, hence it is barely extractible using methanol). These results agree well with other authors findings on *Desmodesmus komarekii* exposed to high light (250 µmolPhotonPAR/m²/s) (Hanagata and Dubinsky 1999). Still, in our case, the later carotenoids are thought to play a role in mitigating ROS species targeting enhanced lipids synthesis products (Zhang et al. 2013). Indeed, under 75 µmolPhotonPAR/m²/s, with low chlorophyll contents, no violaxanthin - meaning xanthophyll cycle downregulation -, light induced ROS production seems unlikely to happen. Furthermore, in our case, the production of storage lipids is confirmed by FAME profiling.

4.3 FAME profile

First of all, the obtained FAME profiles are in agreement with those found in the literature for similar microalgae (Wiltshire et al. 2000). In addition, amounts are within well established range (3 to 60 %g/gDW (Morris et al. 2008; Gris et al. 2014; Vadiveloo et al. 2015)). Still, in our photobioreactor runs the total amount is around 10 %g/gDW, while an increase could have been expected. This can be explained by the fact that nitrogen deficient samples were chosen among those in late exponential (or early stationary) phase. This procedure left only a limited amount of time for the strain to accumulate lipids (Gifuni et al. 2019), yet profile modification is observed, which was the objective. Furthermore, 1-month nitrogen starvation allowed for longer lipid storage build up leading to a doubled strain

lipid content. In any configuration, the three major lipids are oleic acid, linoleic and γ-linolenic acid.

Going one step further, it is possible to determine which lipid is produced commonly or under light or nitrogen stress. As one can see in Table 2, linoleic and oleic acid productions are favoured by low light while γ-linolenic acid is enhanced by high illumination. Higher content of given lipids under low light can be explained by the fact that they might be among the primary targets of light induced ROS (Zhang et al. 2013). Nitrogen deficiency induced appearance (with low amounts) of stearic acid, accumulation of palmitatic and oleic acids while γ-linolenic acid concentration dwindled. Finally, long term (nitrogen starvation) lipid content increase is mainly supported by oleic and linoleic acids. Hence pinpointing them as the storage lipids of this strain.

Oleic acid is a monounsaturated fatty acids with numerous health benefits both as feed and food. As feed, its inclusion in dairy cows diet has been shown to enhance milk production in the most productive cows (Souza et al. 2019). As food, it has demonstrated positive effects in the treatment and prevention of cardiovascular and autoimmune diseases, metabolic disturbance and cancer (Sales-Campos et al. 2013). Linoleic acid is a polyunsaturated fatty acid which shows valuable health properties. Namely, from a metabolic perspective, it improves plasma lipid profile and promotes long-term glycaemic control and insulin resistance (Marangoni et al. 2020). From a population scale perspective, its consumption reduces incidence of cardiovascular diseases, metabolic syndrome and type 2 diabetes (Belury et al. 2018).

Conclusion

Freshwater microalgae *Desmodesmus sp.* has been isolated and profiled under nitrogen sufficient and deficient conditions as well as under regular illumination and light stress. Pigment profiles are common among Chlorophyta phylum, still with natural presence of lutein. Lipid profiling showed that the three main lipids produced by this strain are oleic, linoleic and γ-linolenic acids. While γ-linolenic acid production is enhanced by high illumination, oleic and linoleic acids production is favoured by nitrogen deficiency. Those two last fatty acids have valuable health properties, hence pave the way towards potential biofuel/nutraceutics covalorization of this strain.

Declaration of author contributions

WL, PP and VP initiated and designed the study. WL, MP and VP led the experimental work. CG developed and led the profiling procedure. WL and NG led the photosynthetic apparatuses analysis. The authors critically interpreted the results. VP drafted the manuscript, the other authors corrected it. All authors approve the manuscript.

Conflict of interest

None to disclose.

Acknowledgments

The authors would like to thank Département de la Marne, Région Grand Est, and Grand Reims for their financial support.

References

Acién Fernández, F. G., José María Fernández Sevilla, and Emilio Molina Grima. 2019. "Chapter 21 - Costs Analysis of Microalgae Production." In *Biofuels from Algae (Second Edition)*, edited by Ashok Pandey, Jo-Shu Chang, Carlos Ricardo Soccol, Duu-Jong Lee, and Yusuf Chisti, 551–66. Biomass, Biofuels, Biochemicals. Elsevier. https://doi.org/10.1016/B978-0-444-64192-2.00021-4.

Adams, Curtis, and Bruce Bugbee. 2014. "Nitrogen Retention and Partitioning at the Initiation of Lipid Accumulation in Nitrogen-Deficient Algae." *Journal of Phycology* 50 (2): 356–65. https://doi.org/10.1111/jpy.12167.

Andersen, Robert A., and Phycological Society of America. 2005. *Algal Culturing Techniques*. Academic Press.

Baroli, I., and A. Melis. 1998. "Photoinhibitory Damage Is Modulated by the Rate of Photosynthesis and by the Photosystem II Light-Harvesting Chlorophyll Antenna Size." *Planta* 205 (2): 288–96. https://doi.org/10.1007/s004250050323.

Belury, Martha A., Rachel M. Cole, Deena B. Snoke, Taylor Banh, and Austin Angelotti. 2018. "Linoleic Acid, Glycemic Control and Type 2 Diabetes." *Prostaglandins, Leukotrienes, and Essential Fatty Acids* 132: 30–33. https://doi.org/10.1016/j.plefa.2018.03.001.

Choudhury, N. K., and R. K. Behera. 2001. “Photoinhibition of Photosynthesis: Role of Carotenoids in Photoprotection of Chloroplast Constituents.” *Photosynthetica* 39 (4): 481–88. https://doi.org/10.1023/A:1015647708360.

Enamala, Manoj Kumar, Swapnika Enamala, Murthy Chavali, Jagadish Donepudi, Rajasri Yadavalli, Bhulakshmi Kolapalli, Tirumala Vasu Aradhyula, Jeevitha Velpuri, and Chandrasekhar Kuppam. 2018. “Production of Biofuels from Microalgae - A Review on Cultivation, Harvesting, Lipid Extraction, and Numerous Applications of Microalgae.” *Renewable and Sustainable Energy Reviews* 94 (October): 49–68. https://doi.org/10.1016/j.rser.2018.05.012.

Fasaei, F., J. H. Bitter, P. M. Slegers, and A. J. B. van Boxtel. 2018. “Techno-Economic Evaluation of Microalgae Harvesting and Dewatering Systems.” *Algal Research* 31 (April): 347–62. https://doi.org/10.1016/j.algal.2017.11.038.

Gifuni, Imma, Antonino Pollio, Carl Safi, Antonio Marzocchella, and Giuseppe Olivieri. 2019. “Current Bottlenecks and Challenges of the Microalgal Biorefinery.” *Trends in Biotechnology* 37 (3): 242–52. https://doi.org/10.1016/j.tibtech.2018.09.006.

Gong, Mengyue, and Amarjeet Bassi. 2016. “Carotenoids from Microalgae: A Review of Recent Developments.” *Biotechnology Advances* 34 (8): 1396–1412. https://doi.org/10.1016/j.biotechadv.2016.10.005.

González-Garcinuño, Álvaro, Antonio Tabernero, José M Sánchez-Álvarez, Eva M. Martin del Valle, and Miguel A. Galán. 2014. “Effect of Nitrogen Source on Growth and Lipid Accumulation in Scenedesmus Abundans and Chlorella Ellipsoidea.” *Bioresource Technology* 173 (December): 334–41. https://doi.org/10.1016/j.biortech.2014.09.038.

Griffiths, Melinda J., Clive Garcin, Robert P. van Hille, and Susan T. L. Harrison. 2011. “Interference by Pigment in the Estimation of Microalgal Biomass Concentration by Optical Density.” *Journal of Microbiological Methods* 85 (2): 119–23. https://doi.org/10.1016/j.mimet.2011.02.005.

Gris, Barbara, Tomas Morosinotto, Giorgio M. Giacometti, Alberto Bertucco, and Eleonora Sforza. 2014. “Cultivation of Scenedesmus Obliquus in Photobioreactors: Effects of Light Intensities and LightDark Cycles on Growth, Productivity, and Biochemical Composition.” *Applied Biochemistry and Biotechnology* 172 (5): 2377–89. https://doi.org/10.1007/s12010-013-0679-z.

Guiry, Michael D. 2012. “How Many Species of Algae Are There?” *Journal of Phycology* 48 (5): 1057–63. https://doi.org/10.1111/j.1529-8817.2012.01222.x.

Hanagata, Nobutaka, and Zvy Dubinsky. 1999. “Secondary Carotenoid Accumulation in Scenedesmus Komarekii (Chlorophyceae, Chlorophyta).” *Journal of Phycology* 35 (5): 960–66. https://doi.org/10.1046/j.1529-8817.1999.3550960.x.

Hegewald, Eberhard, Antal Schmidt, Anke Braband, and Petro Tsarenko. 2005. “Revision of the Desmodesmus (Sphaeropleales, Scenedesmaceae) Species with Lateral Spines. 2. The Multi-Spined to Spineless Taxa.” *Algological Studies* 116 (1): 1–38.

Kok, Bessel. 1953. “Chapter 6.” In *Algal Culture from Laboratory to Pilot Plant.*, 63–75. Carnegie Institute Washington Pub.

Lari, Zahra, Narges Moradi-kheibari, Hossein Ahmadzadeh, Parvaneh Abrishamchi, Navid R. Moheimani, and Marcia A. Murry. 2016. “Bioprocess Engineering of Microalgae to Optimize Lipid Production Through Nutrient

Management." *Journal of Applied Phycology* 28 (6): 3235–50. https://doi.org/10.1007/s10811-016-0884-6.

Leonardi, Rodrigo Jorge, Manuel Vicente Ibañez, Matías Nicolás Morelli, Horacio Antonio Irazoqui, and Josué Miguel Heinrich. 2019. "Influence of Light Stratification on the Growth of Scenedesmus Quadricauda." https://pubag.nal.usda.gov/catalog/6394744.

Lim, David KY, and Peer M Schenk. 2017. "Microalgae Selection and Improvement as Oil Crops: GM Vs Non-GM Strain Engineering." *AIMS Bioeng* 4 (1): 151–61.

Liu, Junhan, Cheng Yuan, Guangrong Hu, and Fuli Li. 2012. "Effects of Light Intensity on the Growth and Lipid Accumulation of Microalga Scenedesmus Sp. 11-1 Under Nitrogen Limitation." *Applied Biochemistry and Biotechnology* 166 (8): 2127–37. https://doi.org/10.1007/s12010-012-9639-2.

Mandal, Shovon, and Nirupama Mallick. 2009. "Microalga Scenedesmus Obliquus as a Potential Source for Biodiesel Production." *Applied Microbiology and Biotechnology* 84 (2): 281–91. https://doi.org/10.1007/s00253-009-1935-6.

Marangoni, Franca, Carlo Agostoni, Claudio Borghi, Alberico L. Catapano, Hellas Cena, Andrea Ghiselli, Carlo La Vecchia, et al. 2020. "Dietary Linoleic Acid and Human Health: Focus on Cardiovascular and Cardiometabolic Effects." *Atherosclerosis* 292 (January): 90–98. https://doi.org/10.1016/j.atherosclerosis.2019.11.018.

Masojídek, J., Š. Papáček, M. Sergejevová, V. Jirka, J. Červený, J. Kunc, J. Korečko, et al. 2003. "A Closed Solar Photobioreactor for Cultivation of Microalgae Under Supra-High Irradiance: Basic Design and Performance."

Journal of Applied Phycology 15 (2): 239–48. https://doi.org/10.1023/A:1023849117102.

Mohsenpour, Seyedeh Fatemeh, Bryce Richards, and Nik Willoughby. 2012. "Spectral Conversion of Light for Enhanced Microalgae Growth Rates and Photosynthetic Pigment Production." *Bioresource Technology* 125 (December): 75–81. https://doi.org/10.1016/j.biortech.2012.08.072.

Morris, Humberto J., Angel Almarales, Olimpia Carrillo, and Rosa C. Bermúdez. 2008. "Utilisation of Chlorellavulgaris Cell Biomass for the Production of Enzymatic Protein Hydrolysates." *Bioresource Technology* 99 (16): 7723–9. https://doi.org/10.1016/j.biortech.2008.01.080.

Müller, Patricia, Xiao-Ping Li, and Krishna K. Niyogi. 2001. "Non-Photochemical Quenching. A Response to Excess Light Energy." *Plant Physiology* 125 (4): 1558–66. https://doi.org/10.1104/pp.125.4.1558.

Neofotis, Peter, Andy Huang, Kiran Sury, William Chang, Florenal Joseph, Arwa Gabr, Scott Twary, Weigang Qiu, Omar Holguin, and Jürgen E. W. Polle. 2016. "Characterization and Classification of Highly Productive Microalgae Strains Discovered for Biofuel and Bioproduct Generation." *Algal Research* 15 (April): 164–78. https://doi.org/10.1016/j.algal.2016.01.007.

Ohad, I., N. Adir, H. Koike, D. J. Kyle, and Y. Inoue. 1990. "Mechanism of Photoinhibition in Vivo. A Reversible Light-Induced Conformational Change of Reaction Center II Is Related to an Irreversible Modification of the D1 Protein." *Journal of Biological Chemistry* 265 (4): 1972–9. http://www.jbc.org/content/265/4/1972.

Pancha, Imran, Kaumeel Chokshi, Basil George, Tonmoy Ghosh, Chetan Paliwal, Rahulkumar Maurya, and Sandhya Mishra. 2014. "Nitrogen Stress Triggered

Biochemical and Morphological Changes in the Microalgae Scenedesmus Sp. CCNM 1077." *Bioresource Technology* 156 (March): 146–54. https://doi.org/10.1016/j.biortech.2014.01.025.

Phillips, J. Neal, and Jack Myers. 1954. "Growth Rate of Chlorella in Flashing Light. 1." *Plant Physiology* 29 (2): 152–61. https://www.ncbi.nlm.nih.gov/pmc/articles/PMC540481/.

Přibyl, Pavel, Jan Pilný, Vladislav Cepák, and Petr Kaštánek. 2016. "The Role of Light and Nitrogen in Growth and Carotenoid Accumulation in Scenedesmus Sp." *Algal Research* 16 (June): 69–75. https://doi.org/10.1016/j.algal.2016.02.028.

Ratha, S. K., and R. Prasanna. 2012. "Bioprospecting Microalgae as Potential Sources of "Green Energy"challenges and Perspectives (Review)." *Applied Biochemistry and Microbiology* 48 (2): 109–25. https://doi.org/10.1134/S000368381202010X.

Rizwan, Muhammad, Ghulam Mujtaba, Sheraz Ahmed Memon, Kisay Lee, and Naim Rashid. 2018. "Exploring the Potential of Microalgae for New Biotechnology Applications and Beyond: A Review." *Renewable and Sustainable Energy Reviews* 92 (September): 394–404. https://doi.org/10.1016/j.rser.2018.04.034.

Sales-Campos, Helioswilton, Patricía Reis de Souza, Bethânea Crema Peghini, João Santana da Silva, and Cristina Ribeiro Cardoso. 2013. "An Overview of the Modulatory Effects of Oleic Acid in Health and Disease." *Mini Reviews in Medicinal Chemistry* 13 (2): 201–10.

Sarat Chandra, T., S. Aditi, M. Maneesh Kumar, S. Mukherji, J. Modak, V. S. Chauhan, R. Sarada, and S. N. Mudliar. 2017. "Growth and Biochemical Characteristics of an Indigenous Freshwater Microalga, Scenedesmus Obtusus,

Cultivated in an Airlift Photobioreactor: Effect of Reactor Hydrodynamics, Light Intensity, and Photoperiod." *Bioprocess and Biosystems Engineering* 40 (7): 1057–68. https://doi.org/10.1007/s00449-017-1768-0.

Sati, Himanshu, Madhusree Mitra, Sandhya Mishra, and Prashant Baredar. 2019. "Microalgal Lipid Extraction Strategies for Biodiesel Production: A Review." *Algal Research* 38 (March): 101413. https://doi.org/10.1016/j.algal.2019.101413.

Sforza, Eleonora, Mattia Enzo, and Alberto Bertucco. 2014. "Design of Microalgal Biomass Production in a Continuous Photobioreactor: An Integrated Experimental and Modeling Approach." *Chemical Engineering Research and Design* 92 (6): 1153–62. https://doi.org/10.1016/j.cherd.2013.08.017.

Souza, J. de, N. R. St-Pierre, and A. L. Lock. 2019. "Altering the Ratio of Dietary C16:0 and Cis-9 C18:1 Interacts with Production Level in Dairy Cows: Effects on Production Responses and Energy Partitioning." *Journal of Dairy Science* 102 (11): 9842–56. https://doi.org/10.3168/jds.2019-16374.

Ševčíková, Tereza, Kateřina Bišová, Miloslava Fojtová, Alena Lukešová, Kristýna Hrčková, and Eva Sýkorová. 2013. "Completion of Cell Division Is Associated with Maximum Telomerase Activity in Naturally Synchronized Cultures of the Green Alga Desmodesmus Quadricauda." *FEBS Letters* 587 (6): 743–48. https://doi.org/10.1016/j.febslet.2013.01.058.

Vadiveloo, Ashiwin, Navid R. Moheimani, Jeffrey J. Cosgrove, Parisa A. Bahri, and David Parlevliet. 2015. "Effect of Different Light Spectra on the Growth and Productivity of Acclimated Nannochloropsis Sp. (Eustigmatophyceae)." *Algal Research* 8 (March): 121–27. https://doi.org/10.1016/j.algal.2015.02.001.

Van Wychen, S, and LML Laurens. 2013. “Determination of Total Lipids as Fatty Acid Methyl Esters (FAME) by in Situ Transesterification.” *Contract* 303: 375–00.

Walker, David Alan. 2009. “Biofuels, Facts, Fantasy, and Feasibility.” *Journal of Applied Phycology* 21 (5): 509–17. https://doi.org/10.1007/s10811-009-9446-5.

Wiltshire, Karen H., Maarten Boersma, Anita Möller, and Heinke Buhtz. 2000. “Extraction of Pigments and Fatty Acids from the Green Alga Scenedesmus Obliquus (Chlorophyceae).” *Aquatic Ecology* 34 (2): 119–26. https://doi.org/10.1023/A:1009911418606.

Zhang, Yun-Ming, Hui Chen, Chen-Liu He, and Qiang Wang. 2013. “Nitrogen Starvation Induced Oxidative Stress in an Oil-Producing Green Alga Chlorella Sorokiniana C3.” *PLOS ONE* 8 (7): e69225. https://doi.org/10.1371/journal.pone.0069225.

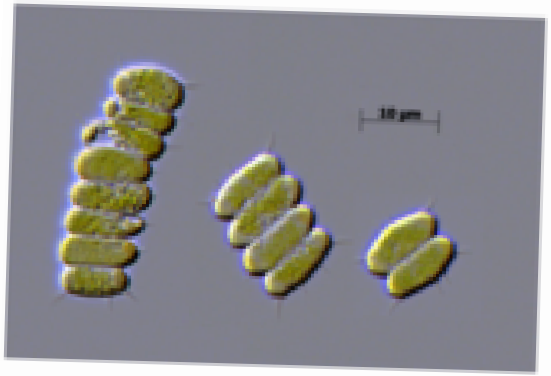

Desmodesmus sp.

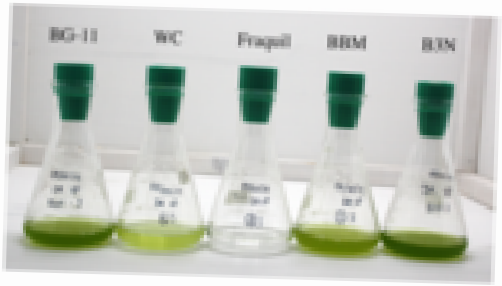

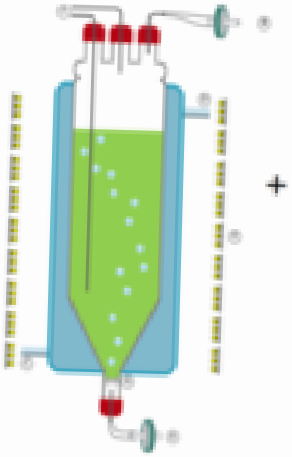

CO2

\+ *Light stress*

Nitrogen stress

Media screening
Nitrogen affinity

Lipid & pigment profiles

Identification of valuable lipids

Potential biofuel covalorization